ISIJ International, Vol. 32 (1992), No. 1, pp. 19–25

Review

Wetting and Marangoni Effect in Iron and Steelmaking Processes

Kusuhiro MUKAI

Department of Materials Science and Engineering, Faculty of Engineering, Kyushu Institute of Technology, Sensui-cho, Tobata-ku, Kitakyushu, Fukuoka-ken, 804 Japan.

(*Received on July 1, 1991; accepted in final form on September 20, 1991*)

This article reviews the phenomena by which wetting and the Marangoni effect participate or may participate in iron and steelmaking processes. The concept of wetting conventionally defined for the system of gas–liquid–solid was applied to the systems of liquid 1–liquid 2–solid, liquid–solid 1–solid 2 and gas–liquid 1–liquid 2. In these systems, local corrosions of refractories at the interfaces of gas–slag and metal–slag, slag foaming, bubble dispersion into metal phase, and interaction of inclusions with solidification fronts were described in relation to the wetting and the Marangoni effect. Rates of reactions of gas–metal, and metal–slag were briefly introduced as examples of possible participation of the Marangoni effect.

KEY WORDS: wetting; Marangoni effect; iron and steelmaking; local corrosion; refractory; slag foaming; bubble dispersion; inclusion; rate of heterogeneous reaction.

1. Introduction

The subject of surface phenomena in relation to iron and steelmaking processes has recently been one of the most attractive fields in metallurgy, which may be because of the following: (1) Further understanding of the kinetics in heterogeneous reactions in metallurgical systems requires more detailed information on surface phenomena that occur during the progress of these reactions. These phenomena can reveal more of the microscopic stages of kinetics than did the conventional treatments used in previous studies. (2) Smelting and refining processes developed or improved recently often include various dispersion actions such as the injection of powder agents into liquid steel, degassing of liquid steel with RH, bubble injection through porous plug refractories and slag foaming in bath smelting or during pre-treatment of pig iron in torpedo cars. Control of non-metallic inclusion during the steel refining process is important for the production of much higher quality steels. Detailed information on surface phenomena is essential to advance practical operations in above processes.

Here, wetting and the Marangoni effect pointed out as important surface phenomena which do or may participate in kinetics of the heterogeneous reactions and/or the practical iron and steelmaking processes. Rather detailed descriptions are given for those phenomena substantiated experimentally, and brief comments made on those not yet experimentally clarified but which appear interesing for studies in the near future.

1.1. Wetting

Wetting of solid (S) by liquid (L) is characterized by contact angle θ as shown in **Fig. 1**, or with the quantity of Helmholtz energy changes for wettings shown in **Fig. 2** and Eqs. (1) to (3).

$$W_s=\sigma_{SG}-\sigma_{LG}-\sigma_{SL} \quad \text{.........................(1)}$$

$$W_i=\sigma_{SG}-\sigma_{SL} \quad \text{.................................(2)}$$

$$W_a=\sigma_{LG}+\sigma_{SG}-\sigma_{SL} \quad \text{........................(3)}$$

where G means gas phase and σ_{ij} is the interfacial tension between phases i and j. Modes of wetting, (a), (b) and (c) in Fig. 2, correspond to spreading wetting, immersional wetting and adhesional wetting, respectively. W_a is the work of adhesion. Equations (5) to (7) are derived from Eqs. (1) to (3) when Young's equation[1] (Eq. (4)) can be applied to the systems in Fig. 2.

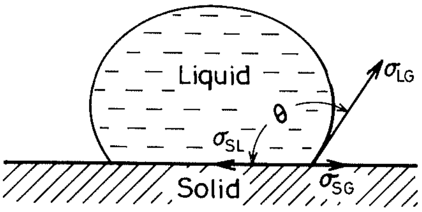

Fig. 1. Contact angle θ and interfacial tensions σ_{ij} for the system of gas–liquid–solid.

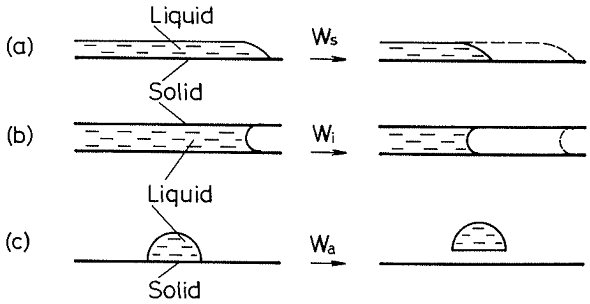

Fig. 2. Three types of wetting for gas–liquid–solid system.

$$\sigma_{SG}=\sigma_{SL}+\sigma_{LG}\cos\theta \qquad (4)$$

$$W_s=\sigma_{LG}(\cos\theta-1) \qquad (5)$$

$$W_i=\sigma_{LG}\cos\theta \qquad (6)$$

$$W_a=\sigma_{LG}(1+\cos\theta) \qquad (7)$$

Equations (5) to (7) are valuable for practical use because σ_{LG} and θ can be determined experimentally.

Analogous treatments to those described above for the system of gas–liquid–solid also may apply to the systems cormposed of various combinations of three different phases: liquid 1–liquid 2–solid, gas–liquid 1–liquid 2, *etc.* Wettings in these three-phase systems are described in relation to the kinetics and metallurgical processes in Chap. 2.

1.2. Marangoni Effect

Surface (or interfacial) tension difference or gradient on the surface (or interface) of liquid, for example, in the direction x, can change the motion of liquid due to the surface shear stress τ_s, written as

$$\tau_s=\frac{d\sigma}{dx}=\frac{\partial\sigma}{\partial T}\cdot\frac{dT}{dx}+\frac{\partial\sigma}{\partial c}\cdot\frac{dc}{dx}+\frac{\partial\sigma}{\partial\psi}\cdot\frac{d\psi}{dx} \qquad (8)$$

Equation (8) indicates that surface (or interfacical) tension tension gradient is caused by the gradients of temperature T, concentration c of the surface active component in the liquid and electric potential ψ at the interface between two liquids.

In hydrodynamics, the surface (or interfacial) tension difference or gradient participating in the above dynamics is called the Marangoni effect.[2] Motions of liquid induced by the Marangoni effect, which is called Marangoni flow or Marangoni convection, are most intensive at the surface or the interface. There the motion can effectively promote both the mass transport and heat transport across the interface. Liquid metals and slags generally have high surface or interfacial tension and also have strong surface active components such as oxygen and sulfur in liquid iron,[3] both factors favorable to the occurrence of Marangoni flow in systems in which these are present.

Even in the field of gravity on the earth, occurrences of the Marangoni effect have been observed in the following systems: 1) Marangoni convection of molten salts and slags due to temperature gradient,[4] 2) spreading and shrinking of slag droplets on the metal due to changes in applied potential,[5] and 3) Marangoni flow of slag film due to concentration gradient, which will be described in further detail in Chap. 3.

2. Wetting in Iron and Steelmaking Processes

2.1. Gas–Liquid–Solid Systems

Wetting of solid by liquid participates or may participate in various metallurgical processes. Mukai *et al.*[6–11] have substantiated that local corrosions of refractories such as oxides and trough materials by liquid slag at the slag surface are caused by active motion of slag film which is formed on the refractory surface above the slag level due to good wettability between the refractories and the liquid slags. The slag film motion is induced by the Marangoni effect, as described in Chap. 3.

Fritz[12] reported that under conditions close to static equilibrium, bubble size detached from a solid surface immersed in liquid was predominantly affected by contact angle θ between the solid and the liquid. Ogino and Nishiwaki[13] showed experimentally that the Fritz treatment was applicable to the system of CO bubble–liquid slag–solid SiC. Mukai *et al.*[14] found that even at high gas velocity, u_G through the orifice of $5\,\text{m/sec}\leq u_c\leq 15\,\text{m/sec}$, bubble size detached from the orifice plate immersed in liquid increased with increasing contact angle θ between the plate material and the liquid (**Fig. 3**). Bubble volume V_B (cm^3) detached from the orifice plate can be described by Eq. (9) obtained experimentally by Davidson and Amick[15] when orifice diameter d_o (cm) in Eq. (9) is replaced by d_{1m}, the maximum diameter of the periphery of a bubble adhering to the plate during its growth stage.

$$V_B=0.0824\,(V_G d_o^{0.5})^{0.867} \qquad (9)$$

where V_G is gas flow rate (cm^3/sec). d_{1m} increases with increasing θ, resulting in an increase in the bubble volume V_B as predicted from Eq. (9). Sano and his colleagues[16,17] showed that V_B could be well described by Eq. (9) when the outer diameter of the nozzle was used for d_o in the systems of gas–mercury–silica (nozzle) and gas–liquid iron–alumina (nozzle), where wettability between the liquid metal and nozzle materials was very poor. Ozawa *et al.*[18] showed that a decrease in the distance between two neighboring orifices in the liquid promoted the coalescence of adjacent bubbles formed from them. When bubbles are formed, for example, on the porous plug refractory, an increase in d_{1m} due to poor wettability between liquid steel and the porous plug consisting of solid oxide leads to the coalescence of adjacent bubbles on the surface of the plug. This coalescence may result in the formation of large bubbles in liquid steel. Glass–water systems may simulate the formation of large bubbles in the system of liquid

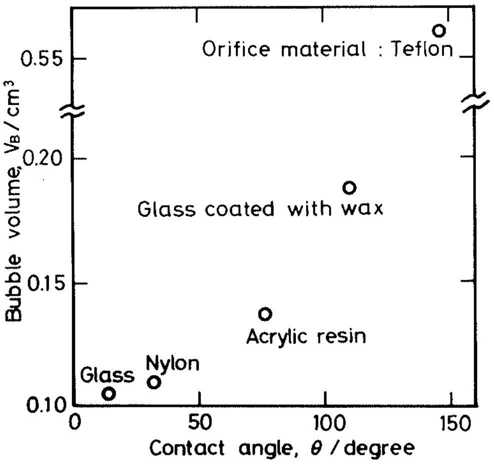

Fig. 3. Relation between bubble volume detached from plate orifice in water and contact angle between plate material and water at 298 K.[14] $u_G=5\,\text{m/sec}$, $d_o=0.8\,\text{mm}$.

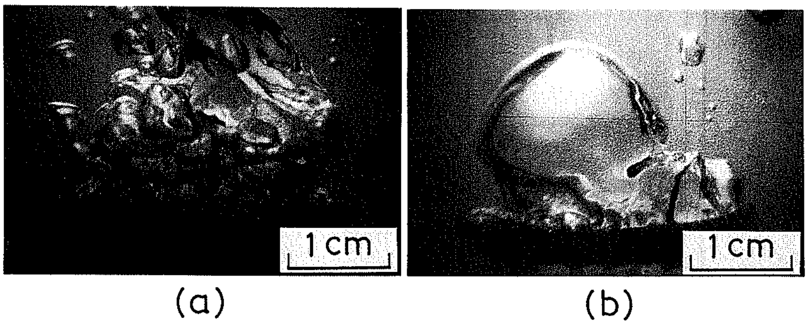

Fig. 4. Dispersion modes of gas into water from glass filters with different wettabilities by water at 298 K.[14] $V_G = 33\,\mathrm{cm}^3/\mathrm{s}$ and porosity of glass filter is equal to 50%. (a): clean glass filter, (b): glass filter coated with wax.

steel–porous plug, as shown in **Fig. 4** where large bubbles are formed on the glass filter coated with wax ($\theta = 109°$) immersed in water, while small bubbles have detached themselves from the clean glass filter ($\theta = 14°$).

Ebisawa *et al.*[19] showed that the reduction rate of (SiO_2) with graphite can be increased by good wettability of the graphite with liquid slag, due primarily to the increase in interface area between the two materials with decreasing θ.

Uchimura *et al.*[20] have indicated that the main cause of nozzle clogging with inclusions in continuous casting of liquid steel is thought to be poor wettability between the liquid steel and both inclusions and oxides of the nozzle material.

2.2. Liquid 1–Liquid 2–Solid Systems

We can apply the concept of wetting described in Sec. 1.1 to the system of liquid metal–liquid slag–solid oxide, where the gas phase in Sec. 1.1 is replaced by liquid metal.

Mukai *et al.*[21,22] have clarified that liquid slag penetrates into the region between liquid lead and solid silica. The penetration in this system corresponds to the spreading wetting shown in case (a) in Fig. 2. Slag film formed by the penetration between liquid lead and solid silica moves actively due to the Marangoni effect, resulting in local corrosion of solid silica at the metal–slag interface. Details of local corrosion will be described in Sec. 3.2.

It was substantiated by Mukai *et al.*[23–25] that local corrosion of trough materials occurred at the metal–slag interface in essentially the same manner as that in the liquid lead–liquid slag–solid silica system, though reactions of slag–carbon in the metal and slag film–SiC in the trough material, *etc.* had a rather complexed effect on the local corrosion.

Mukai *et al.*[26] also clarified a process in which local corrosion of an immersion nozzle occurs at the interface between liquid metal and slag. As shown in Fig. 5, when the wall of nozzle material is initially covered with a slag film (**Fig. 5(a)**), the film not only wets the oxides, but dissolves them in preference to graphite. This changes the interface to a graphite-rich layer. Since the metal phase wets graphite better than the slag, the metal phase creeps up the surface of the specimen as indicated in **Fig. 5(b)** and dissolved graphite in preference to the oxides. Once the graphite-rich layer disappears due to dissolution into metal, the slag can again penetrate the boundary between the metal and the specimen, and the process is repeated. This cycle produces a local corrosion zone at the metal–slag interface.

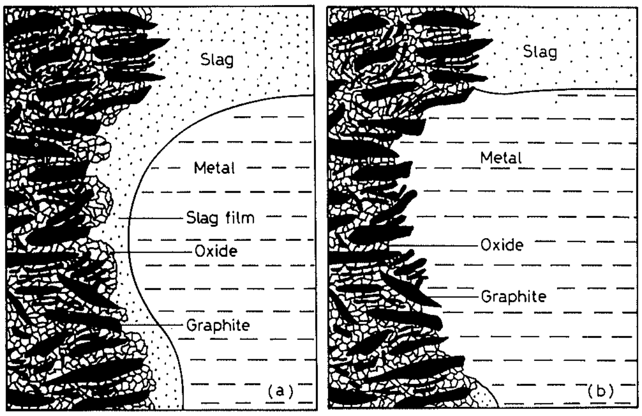

Fig. 5. Schematic representation of the manner in which local corrosion of immersion nozzle proceeds.[26]

2.3. Liquid–Solid 1–Solid 2 Systems

The interaction of inclusions with solidification fronts is a phenomenon of interest for controlling the distribution of inclusions in solidified steel. It is expected that at a low rate of solidification, inclusions may be engulfed by the solidification front if the free energy of engulfing

$$\Delta F^{\mathrm{eng}} = \sigma_{IS} - \sigma_{IL} \qquad \text{(10)}$$

is negative,[27] where I and S mean inclusion and solid metal, respectively. ΔF^{eng} corresponds to the quantity, $-W_i$ in Eq. (2), though the value ΔF^{eng} is difficult to measure. Omenyi and Neumann[27,28] substantiated the following: 1) in systems of liquid organic–polymer (particle), particles are engulfed by solidification fronts when $\Delta F^{\mathrm{eng}} < 0$ at low solidification rate; 2) even if $\Delta F^{\mathrm{eng}} > 0$, particles can be engulfed at higher solidification rate; and 3) the critical solidification rate that enables the solidification front to engulf particles decrease with increasing diameter of a particle. Their treatments[27,28] are applicable to the system of liquid metal–solid metal–solid inclusion.

2.4. Gas–Liquid 1–Liquid 2 Systems

The main cause of slag foaming in iron and steelmaking processes is considered to be the high speed evolution of fine CO bubbles from the interface between slag and metal due to metal–slag reaction.[29] Mukai and Nakamura[30] analyzed precisely the bubble shape and its maximum adherence volume on the interface between two liquids. Their analysis and experiments of electrolysis using a water solution–mercury system revealed that 1) it is the contact angle θ (shown in **Fig.**

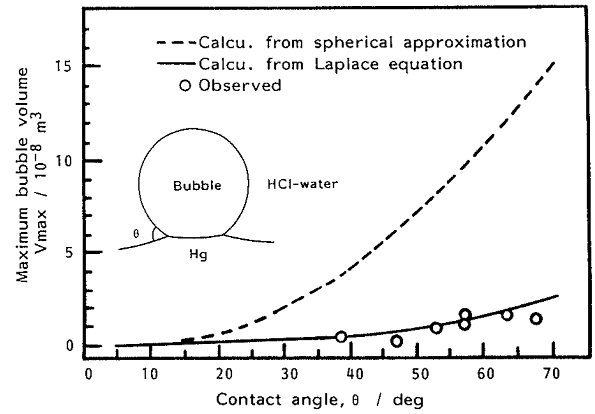

Fig. 6. Relation between maximum bubble volume and contact angle between mercury and hydrochloric acid–water solution.[30]

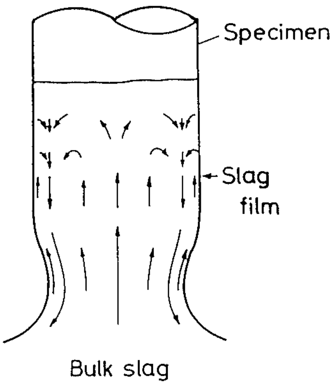

Fig. 7. Typical flow pattern of slag film on a silica rod with 6 mm OD.[7]

6) that predominantly determines the maximum bubble size which can adhere to the interface, and 2) the maximum predicted bubble volume from their analysis taking account of contact angle θ agrees with the observed value, which is much smaller than that predicted from the balance between surface tension and buoyancy when shape of the bubble is other than a sphere.

Shibata *et al.*[31] proposed that, the rate of reaction (11) could be affected by the morphology of CO bubbles formed at the metal–slag interface from this reaction

$$(\mathrm{FeO})+\underline{\mathrm{C}}=\mathrm{CO(g)}+\mathrm{Fe(l)} \quad \text{.........................}(11)$$

3. Marangoni Effect in Iron and Steelmaking Processes

3.1. Gas–Liquid–Solid Systems

Section 2.1 states that local corrosion of solid oxide at the slag surface is caused by Marangoni flow of slag film formed on the surface of solid oxide.[6–10]

The slag film flow in the local corrosion zone is principally composed of whide zones of rising film and narrow zones of falling film in the the system of (PbO–SiO_2) slag–SiO_2(s) (**Fig. 7**). The upper film of rising zone has higher SiO_2 content than the lower film, which causes a surface tension gradient resulting in Marangoni flow of the slag film. Hydrodynamic analysis well explains the observed slag film motion. Velocity distribution in the slag film obtained from the analysis (**Fig. 8**) shows that the slag film motion in the local corrosion zone is still active even in a thin slag film with a thickness of several tens of μm. The film has a concentration gradient of SiO_2 perpendicular to the surface of the solid silica, which means that a diffusion layer has been formed over the whole range of the slag film. The Marangoni flow in the slag film therefore results in breakdown of the diffusion layer, which is the main cause of local corrosion. In other words, local corrosion proceeds largely as a result of the washing of the wall of solid silica with a fresh thin rising slag film induced by the Marangoni effect. The corner of a prism specimen that is continuously washed only by the rising film, as shown in **Fig. 9**, is thus corroded much faster than the plane side, which leads to the formation of a round shape of horizontal cross section of the specimen from the initial square shape. On the other hand, a cylindrical specimen retains its initial round shape of horizontal cross section in the local corrosion zone, because the rising zone of the slag film shifts its location with time horizontally on the surface of the specimen, resulting in an almost even corrosion rate at the same level in the local corrosion zone.

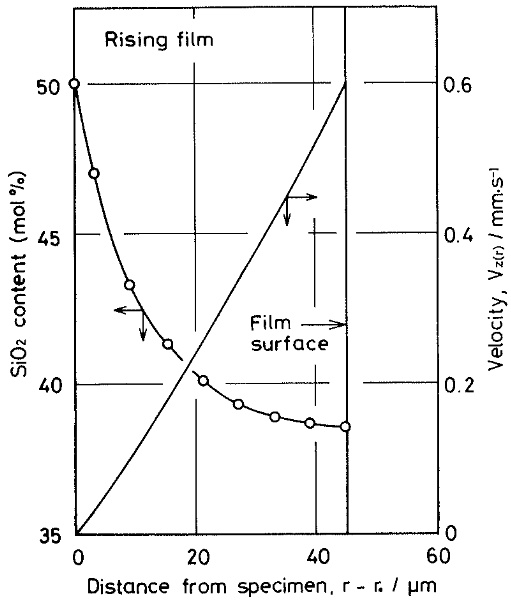

Fig. 8. Distributions of velocity and SiO_2 content in the slag film for a 6 mm OD silica rod dipped for 0.3 ks in 30 mol% SiO_2 slag at 1 073 K.[8]

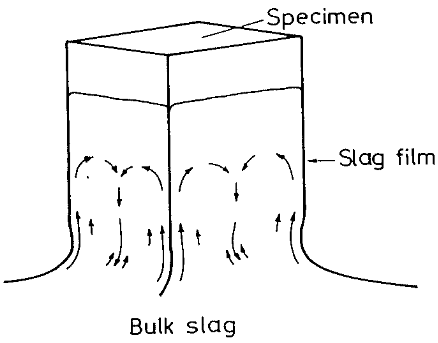

Fig. 9. Typical flow pattern of slag film on a prism silica specimen 6 mm square.[7]

Trough materials composed mainly of oxides and SiC,

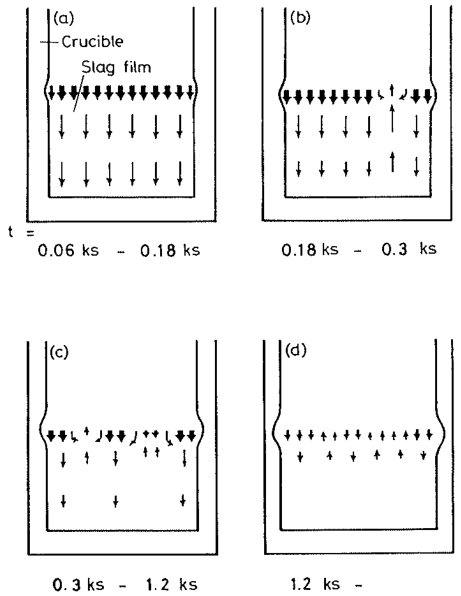

Fig. 10. Schematic representation of flow pattern of slag film formed between liquid lead and silica crucible.[22] *t*: elapsed time after the formation of the film.

which have good wettability with liquid slag, are also corroded locally at the gas–slag interface in an oxidizing atmosphere. Mukai *et al.*[11] clarified that the mechanism of the local corrosion for this system is essentially similar to that for the system of (PbO–SiO_2) slag–SiO_2(s) described above. SiC in the trough material is oxidized into SiO_2 with oxygen supplied through the slag film from the oxidizing atmosphere. The oxidized SiO_2 dissolves in the slag film, which causes concentration gradient on the surface of the slag film in a vertical direction, resulting in local corrosion by the Marangoni flow of the slag film.

3.2. Liquid 1–Liquid 2–Solid System

Mukai *et al.*[21,22] proved that the Marangoni flow of the slag film in the local corrosion zone of a Pb(l)–(PbO–SiO_2) slag–SiO_2(s) system is induced by the concentration gradient of SiO_2 in the film at the interface between liquid lead and slag film in the vertical direction (**Fig. 10**). The slag film motion was observed directly through the wall of a transparent silica crucible. The figure shows that the flow pattern is composed primarily of a downward flow during the initial stage of the corrosion and then an upward flow of the film increases in its frequency and area with time. The active Marangoni flow of the slag film with a thickness of several tens of μm accelerates the dissolution rate of SiO_2 from the SiO_2 crucible into the film, resulting in local corrosion at the metal–slag interface. The manner in which local corrosion occurs in this system is essentially the same as that for a gas–(PbO–SiO_2) slag–SiO_2(s) system when the phase of liquid lead is replaced with a gas phase and the present system is turned upside down.

The Marangoni flow of slag film in the local corrosion zone of a metal–slag–trough material system is also induced by concentration gradient of the slag film at the interface between the film and the metal in the vertical direction.[23-25] The concentration gradient is caused by several kinds of reactions between the slag film and metal or the film and the trough material, as shown in **Fig. 11**. The reaction (12) partially participates in the promotion of local corrosion by agitating the slag film as CO bubbles evolve.

$$(SiO_2)+2\underline{C} \rightarrow \underline{Si}+CO(g) \qquad (12)$$

Carbon particles generated by reaction (13) are suspended in the slag film and dissolve into metal phase when the carbon concentration in the metal is low, thus accelerating local corrosion.

$$SiC(s)+2(FeO) \rightarrow (SiO_2)+2Fe(l)+C(s) \qquad (13)$$

For metals containing high carbon content (*e.g.*, in the vicinity of carbon saturation), suspended carbon particles remain in the slag film, which prevents motion of the film and reduces the contact area between the film and the metal, resulting in the reduction of local corrosion rate.

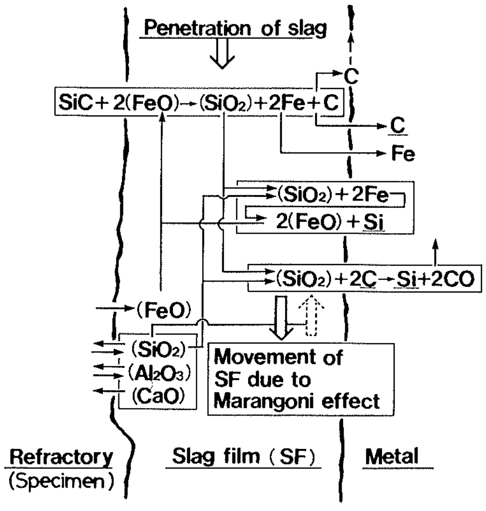

Fig. 11. Transfer paths of reactants and products during the progress of local corrosion of trough material at the slag–metal interface.[25]

The Marangoni flow of the slag film is also considered to play an important role in the local corrosion of immersion nozzles at the metal–slag interface during the stage of Fig. 5(a).[26]

3.3. Gas–Liquid and Liquid 1–Liquid 2 Systems

When surface active components are transferred across a gas–metal or metal–slag interface, their rates of transfer often change and the Marangoni flow is believed to occur at and around the interfaces.

Brimacombe and Weinberg[32] found that when oxygen gas was blown onto the surface of liquid iron, a bright patch of oxide was formed on the surface and small patches of oxide moved at high speed radially from the center patch. The high speed flow was estimated to occur due to the Marangoni effect.

Mizukami *et al.*[33] found that rates of nitrogen removal from liquid steel to gas phase were increased by the flushing of hydrogen gas onto the surface of liquid steel. This increase in rate was thought to be caused by the fluid flow on the surface of liquid steel induced by the Marangoni effect.

Yamamoto and Kato[34] reported that when tin, a surface active element, was evaporated from liquid Fe–Sn alloys under vacuum, surface movement of the liquid alloy was observed and the mass transfer coefficient of tin was increased. The surface movement was believed to be caused by the Marangoni effect.

Sahoo *et al.*[35] found that rates of vaporization of iron drops were enhanced when oxygen or sulfur was present in the drops. This rate increase was considered to be consistent with the interfacial turbulence caused by the surface active elements.

Mukai and Shinozaki[36] have shown that flow direction and geometry of metal pools formed in an iron specimen by plasma arc change with oxygen content of the specimen. These changes are well explained by the Marangoni flow in the pool. Since the center surface of the metal pool has a higher temperature than the periphery of the pool, surface tension at this surface is lower than that at the periphery when oxygen content of the pool is lower than about 0.01 mass% (**Fig. 12**). This surface tension gradient induces outward flow at and around the surface of the pool, resulting in a broad and shallow pool due to preferential heat transfer in a horizontal direction by the outward flow. When oxygen content is higher than 0.01 mass%, reverse flow is induced owing to the positive temperature coefficient of surface tension shown in Fig. 12, which leads to a narrow and deep pool. **Figure 13** shows a clear linear relation between temperature coefficient of surface tension and geometry of the metal pool, that is, the ratio of depth to width. This result indicates that the Marangoni flow predominantly influences the geometry of a metal pool.

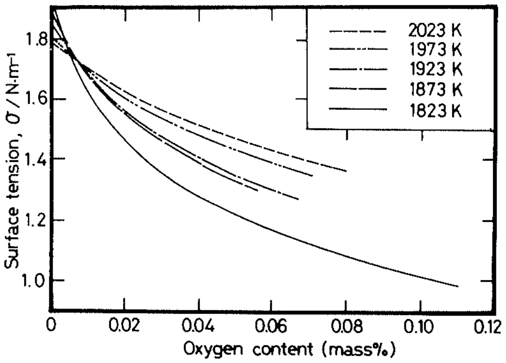

Fig. 12. Effect of oxygen content in liquid iron on surface tension at various temperatures.[36]

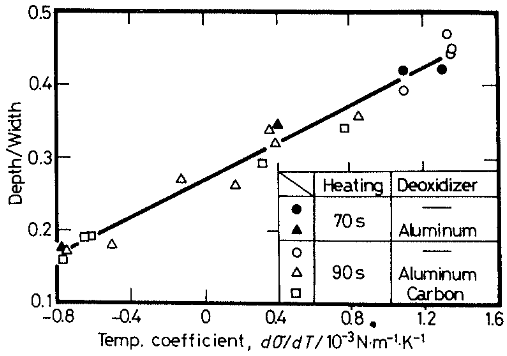

Fig. 13. Relation between temperature coefficient of surface tension and the ratio of depth to width of a molten pool formed in an iron specimen.[36]

In metal–slag systems, Riboud and Lucas[37] stated that interfacial flow was likely to occur due to interfacial tension gradient when metal–slag reactions such as desulfurization were in progress; they based this on their observation of the metal–slag interface using a high temperature X-ray radiographic technique.

Kawai *et al.*[38] also indicated the possibility of weak interfacial turbulence for the case of manganese transfer across the metal–slag interface from their observation of blurred images of the interface outline using an X-ray technique.

Saelim and Gaskell[39] found that rates of desulfurization of Fe–O–S melts by lime saturated liquid iron oxide were significantly greater than that calculated on the assumption of diffusion control in the metal phase. They presented evidence in support of the speculation that the reaction rate was enhanced by the Marangoni flow at the metal–slag interface.

Deng and Oeters[40] found that mass-transfer coefficients of sulfur from liquid iron into lime saturated slag became larger with increasing sulfur content of metal under defined flow conditions of liquid metal induced by gas stirring. This is interpreted as mass transfer by interfacial convection superimposed on normal mass transfer. They showed the eruptions formed at the interface of metal droplets emulsified in slag as evidence of interfacial convection.

4. Concluding Remarks

The present brief review has shown that wetting and the Marangoni effect participate in various processes in iron and steelmaking. More substantial experiments and more quantitative analyses may reveal additional phenomena or processes in which these two factors participate, and these, in turn, will lead to innovative developments in the iron and steelmaking processes.

For this purpose, it is initially necessary to measure various quantities of surface chemistry such as surface tension, interfacial tension, and contact angle, under the same conditions in which surface phenomena or processes in iron and steelmaking take place, for example, surface tension or interfacial tension under a non-equilibrium state during the progress of reactions, and contact angles during advance or recession for the various systems listed in Chap. 2. Also, the surface chemistry data mentioned above is lacking in the systems containing liquid steels, slags and refractories for practical use. Contribution of wetting or the Marangoni effect on the processes should also be clarified separately from other factors. At the present stage of surface chemistry at high temperatures it is of particular importance to substantiate the occurrence of the Marangoni effect in various processes before investigating its contribution.

REFERENCES

1) T. Young: *Philos. Trans. R. Soc. (London)*, **95** (1805), 65.

2) R. Bruckner: *Glastech. Ber.*, **53** (1980), 77.

3) B. J. Keene: *Int. Mater. Rev.*, **33** (1988), 1.

4) T. Nakamura, K. Yokoyama, F. Noguchi and K. Mukai: *CAMP-ISIJ*, **3** (1990), 100.

5) K. Mukai, J. M. Toguri, I. Kodama and J. Yoshitomi: *Can. Metall. Q.*, **25** (1986), 225.

6) K. Mukai, A. Iwata, T. Harada, J. Yoshitomi and S. Fujimoto: *J. Jpn. Inst. Met.*, **47** (1983), 397.

7) K. Mukai, T. Nakano, T. Harada, J. Yoshitomi and S. Fujimoto: Proc. 2nd Int. Symp. Metallurgical Slags and Fluxes, Met. Soc. AIME, Pennsylvania, (1984), 207.

8) K. Mukai, T. Harada, T. Nakano and K. Hiragushi: *J. Jpn. Inst. Met.*, **49** (1985), 1073.

9) K. Mukai, T. Harada, T. Nakano and K. Hiraguchi: *J. Jpn. Inst. Met.*, **50** (1986), 63.

10) T. Harada, S. Fujimoto, A. Iwata and K. Mukai: *J. Jpn. Inst. Met.*, **48**, (1984), 181.

11) K. Mukai, T. Masuda, J. Yoshitomi, T. Harada and S. Fujimoto: *Tetsu-to-Hagané*, **70** (1984), 823.

12) W. Fritz: *Pysik. Z.*, **36** (1935), 379.

13) K. Ogino and A. Nishiwaki: *Tetsu-to-Hagané*, **65** (1979), 1985.

14) K. Mukai, H. Nozaki and T. Arikawa: *CAMP-ISIJ*, **3** (1990), 137.

15) L. Davidson and E. H. Amick, Jr.; *A. I. Ch. E. J.*, **2** (1956), 337.

16) M. Sano and K. Mori: *Tetsu-to-Hagané*, **60** (1974), 348.

17) M. Sano, K. Mori and T. Sato: *Tetsu-to-Hagané*, **63** (1977), 2308.

18) Y. Ozawa, Y. Matsui, K. Mori and M. Sano: *Tetsu-to-Hagané*, **73** (1987), 1543.

19) Y. Ebisawa, M. Tokuda and M. Ohtani: Final Report of the Committee of Blast Furnace Process and its Modelling, ISIJ, Tokyo, (1982), 227.

20) M. Uchimura, S. Ogibayashi, K. Yamaguchi, H. Honma and H. Yamaguchi: *CAMP-ISIJ*, **4** (1991), 219.

21) K. Mukai, T. Masuda, K. Gouda, T. Harada, J. Yoshitomi and S. Fujimoto; *J. Jpn. Inst. Met.*, **48** (1984), 726.

22) K. Mukai, K. Gouda, J. Yoshitomi and K. Hiragushi: Proc. 3rd Int. Conf. on Molten Slags and Fluxes, The Inst. of Met., London, (1989), 215.

23) K. Mukai, T. Masuda, J. Yoshitomi, T. Harada and S. Fujimoto: *Tetsu-to-Hagané*, **70** (1984), 823.

24) J. Yoshitomi, T. Harada, K. Hiragushi and K. Mukai: *Tetsu-to-Hagané*, **72** (1986), 411.

25) J. Yoshitomi, K. Hiragushi and K. Mukai: *Tetsu-to-Hagané*, **73** (1987), 1535.

26) K. Mukai, J. M. Toguri, N. M. Stubina and J. Yoshitomi: *ISIJ Int.*, **29** (1989), 469.

27) S. N. Omenyi and A. W. Neumann: *J. Appl. Phys.*, **52** (1981), 789.

28) S. N. Omenyi and A. W. Neumann: *J. Appl. Phys.*, **47** (1976), 3956.

29) K. Mukai: *Tetsu-to-Hagané*, **77** (1991), 856.

30) K. Mukai and T. Nakamura: Interfacial Transport Phenomena in Pyrometallurgical Processes, ed. by Comm. on Interfacial Transport Phenomena, The Joint Soc. on Iron and Steel Basic Research, ISIJ, Tokyo, (1991), 36.

31) K. Shibata, T. Kitamura and N. Tokumitsu: *Tetsu-to-Hagané*, **76** (1990), 2011.

32) J. K. Brimacombe and F. Weinberg: *Metall. Trans.*, **3** (1972), 2298.

33) Y. Mizukami, S. Mukawa, T. Saeki, H. Shima, S. Onoyama, T. Komai and S. Takaishi: *Tetsu-to-Hagané*, **74** (1988), 294.

34) M. Yamamoto and E. Kato: *Tetsu-to-Hanagé*, **66** (1980), 608.

35) P. Sahoo, M. M. Collur and T. Derbroy: *Metall. Trans.*, **19B** (1988), 967.

36) K. Mukai and S. Shinozaki: Interfacial Transport Phenomena in Pyrometallurgical Processes, ed. by Comm. on Interfacial Transport Phenomena, The Joint Soc. on Iron and Steel Basic Research, ISIJ, Tokyo, (1991), 193.

37) P. V. Riboud and L. D. Lucas: *Can, Metall. Q.*, **20** (1981), 199.

38) Y. Kawai, N. Shinozaki and K. Mori: *Can. Metall. Q.*, **21** (1982), 385.

39) A. Saelim and D. R. Gaskell: *Metall. Trans.*, **14B** (1983), 259.

40) J. Deng and F. Oeters: *Steel Res.*, **61** (1990), 438.